Microelectronic Engineering 87 (2010) 2525–2530

Contents lists available at ScienceDirect

Microelectronic Engineering

journal homepage: www.elsevier.com/locate/mee

Extraction of electronic parameters of Schottky diode based on an organic Orcein

Şakir Aydoğan [a,*], Ümit İncekara [b], A.R. Deniz [a], Abdulmecit Türüt [a]

[a] Department of Physics, Faculty of Sciences, Atatürk University, 25240 Erzurum, Turkey
[b] Department of Biology, Faculty of Sciences, Atatürk University, 25240 Erzurum, Turkey

ARTICLE INFO

Article history:
Received 18 February 2010
Received in revised form 3 June 2010
Accepted 7 June 2010
Available online 11 June 2010

Keywords:
Schottky barrier height
Orcein
Organic materials
Ideality factor
Capacitance measurements

ABSTRACT

An Au/Orcein/*p*-Si/Al device was fabricated and the current–voltage measurements of the devices showed diode characteristics. Then the current–voltage (*I–V*), capacitance–voltage (*C–V*) and capacitance–frequency (*C–f*) characteristics of the device were investigated at room temperature. Some junction parameters of the device such as ideality factor, barrier height, and series resistance were determined from *I–V* and *C–V* characteristics. The ideality factor of 2.48 and barrier height of 0.70 eV were calculated using *I–V* characteristics. It has been seen that the Orcein layer increases the effective barrier height of the structure since this layer creates the physical barrier between the Au and the *p*-Si. The interface state density N_{ss} were determined from the *I–V* plots. The capacitance measurements were determined as a function of voltage and frequency. It was seen that the values of capacitance have modified with bias and frequency.

1. Introduction

It is well known that metal/semiconductor (MS) contacts or organic/inorganic semiconductor structures [1,2] are of great importance since they are present in most semiconductor device. Recently, metal oxides such as Cu_2O, strontium titanate oxide (STO) and Gd_2O_3 have been also deliberately deposited using pulsed laser deposition technique on silicon substrate to study these junction properties [3–5]. The past decade has witnessed tremendous advances in the development of organic conductive molecular and polymeric materials and this field continues to be of great scientific and commercial interest. Furthermore, recently, extensive researches have been carried out for applying semiconducting organic materials to electronic devices such as organic light emitting diodes, Schottky diodes based on organic materials, organic solar cells and organic field effect transistors. Thus, semiconducting organic materials can be used in various condensed matter physics applications. It is well known that the interfacial properties of metal/semiconductor (MS) contacts have a dominant influence on device performance, reliability and stability. There is a native thin insulating layer of oxide on the surface of the semiconductor in most practical MS contacts. This layer converts the MS structure into a metal/insulator/semiconductor device [2]. Besides, it can be constructed as an organic thin film between metal and inorganic semiconductor intentionally. This organic film modifies some electrical parameters of the devices. For example, Schottky barrier heights of MS contacts can be manipulated by insertion of a dipole layer between the semiconductor and the organic film. Numerous studies of thin films of organic conductors on semiconductors have been performed in order to investigate the electronic properties of various organic materials based on Schottky diodes. Furthermore, so far many attempts have been made to realize a modification and the continuous control of the barrier height using an organic semiconducting layer, an insulating layer and/or a chemical passivation procedure at certain metal/inorganic semiconductor interfaces, or to determine characteristic parameters of organic film [6–10].

It is well known that the interfacial properties of MS contacts have a dominant influence on device performance, reliability and stability. The electronic parameters of the interface may give rise to an increased contact resistance. Therefore, it is important to understand the relationship between the chemical or structural characteristics of the organic materials and metal/semiconductor interface and thus, charge carrier transport in organic materials based on Schottky diodes. For example, the difference in mobility between the top-contact and bottom-contact organic based Schottky diode was associated to the different morphology of the organic layer near the metallic contacts. The device characteristics are dependent upon the anisotropy of the transport properties in the organic thin film. The different layers of the various devices are optimized for the transport of either electrons or holes, or for the efficient photogeneration of charge carriers, or for efficient emission of light. The electrodes either inject or remove charge from the devices and provide electrical contact with other components. Without describing here the details of operation of all of

* Corresponding author. Tel.: +90 442 231 4073; fax: +90 442 236 0948.
E-mail address: saydogan@atauni.edu.tr (Ş. Aydoğan).

0167-9317/$ - see front matter © 2010 Elsevier B.V. All rights reserved.
doi:10.1016/j.mee.2010.06.004

these devices, it should be apparent that efficient charge transfer across the metal–organic interface is critical to their performance. The most important but not the only factor that controls the charge injection process is the energy barrier to be overcome as the charge carrier crosses the interface [11–13].

A thin organic layer can easily be made by low cost methods and appropriate processing allows organic thin films to be produced in large areas. The characteristics of conducting organic material/inorganic semiconductor interfaces have been considered as very important since it has been indicated that restrictions on Schottky barrier devices can be overcome by using conducting organic material contact layers. Besides this, the ability to manipulate the interface characteristics by changing the organic material dopant allows switchable devices to be fabricated. In many cases organic films can be prepared by controlled evaporation onto substrate in vacuum. In other cases, they are formed onto substrate by spin coating method. After evaporation of the solvent, amorphous or partially crystalline or liquid–crystal films are formed, whose thickness can in many cases be varied in a controlled way. The purpose of this work to fabricate an Au/Orcein/*p*-Si/Al Schottky device and investigate the electrical characterizations of the device. Orcein is soluble in water and under certain conditions, it can behave as an amphoteric dye. Amphoteric dyes have both positively chargeable groups and negatively chargeable groups present on the molecule. Depending on the charge actually present, these dyes may interact as either positively charged ions (basic dyes) or negatively charged ions (acid dyes). Its chemical formula is $C_{28}H_{24}N_2O_7$ and it forms dark brown crystals. The molecular structure of the Orcein is given in Fig. 1. In addition to the morphological features of the Orcein layer, the performance of an organic based Schottky diode may be influenced by the microscopic interface environment at the interface between the Orcein layer and Au contact. This study is the first attempt investigating the effects of a thin Orcein organic layer in MS contacts.

2. Experimental procedure

We have used a *p*-type Si semiconductor wafer with (1 0 0) orientation and 400 μm thickness and 1–10 Ω cm resistivity. The wafer was chemically cleaned using the RCA cleaning procedure (i.e. 10 min boil in $NH_3 + H_2O_2 + 6H_2O$ followed by a 10 min $HCl + H_2O_2 + 6H_2O$ at 60 °C) before making contacts. The ohmic contact with a thickness of 200 nm was made by evaporating Al metal on the back of the *p*-Si substrate, then was annealed at 580 °C for 3 min in N_2 atmosphere. The native oxide on the front surface of substrate was removed in $HF + 10H_2O$ solution. Finally, it was rinsed in de-ionized water for 30 s and was dried. Orcein organic layer with a thickness of 80 nm was directly formed on the front surface of the *p*-Si wafer. Then, Au was evaporated on the organic layer at 10^{-5} torr (diode area = 7.85×10^{-3} cm^2). The current–voltage (*I*–*V*) and capacitance–voltage–frequency (*C*–*V*–*f*) measurements of Au/Orcein/*p*-Si/Al structure were performed with KEITHLEY 487 Picoammeter/Voltage Source and HP 4192A (50 Hz-13 MHz) LF IMPEDENCE ANALYZER, respectively at room temperature.

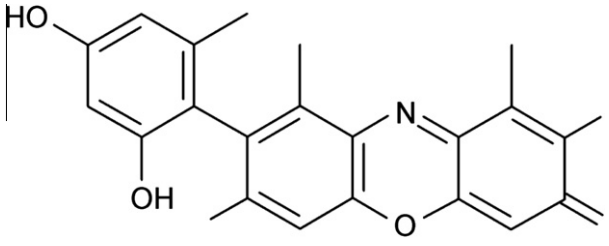

Fig. 1. Chemical structure of Orcein.

3. Results and discussion

The measured *I*–*V* characteristics of the structure have been analyzed using the conventional Schottky barrier thermionic emission theory (TE) [2]

$$I = I_0\left[\exp\left(\frac{qV}{nkT}\right) - 1\right], \tag{1}$$

where

$$I_0 = AA^*T^2 \exp\left(-\frac{q\Phi_b}{kT}\right), \tag{2}$$

is the saturation current, Φ_b is the effective barrier height at zero bias, A^* is the Richardson constant and equals to 32 A cm^{-2} K^{-2} for *p*-type Si, where *q* is the electron charge, *V* is the applied voltage, *A* is the diode area, *k* is the Boltzmann's constant, *T* is the temperature in Kelvin, *n* is the ideality factor, and it is determined from the slope of the linear region of the forward bias ln*I*–*V* characteristic through the relation:

$$n = \frac{q}{kT}\frac{dV}{d(\ln I)}. \tag{3}$$

n equals to 1 for an ideal diode. However, *n* has usually a value greater than unity. High values of *n* can be attributed to the presence of the interfacial thin layer, a wide distribution of low-Schottky barrier height (SBH) patches (or barrier inhomogeneities) and to the bias voltage dependence of the SBH [2]. Φ_b is the zero-bias barrier height (BH), which can be obtained from the following equation:

$$\Phi_b = kT/q \ln\left(AA * T^2/I_0\right). \tag{4}$$

Fig. 2 depicts the current–voltage (log*I*–*V*) characteristics of the Au/Orcein/*p*-Si/Al device. It is shown that the device presents a

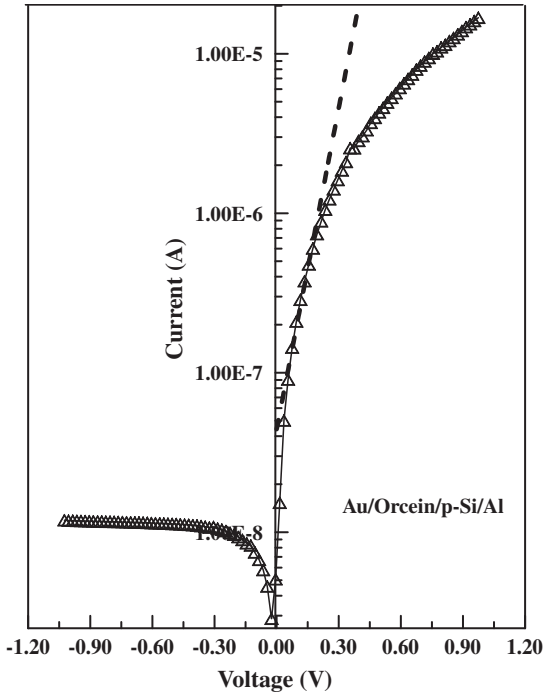

Fig. 2. The current–voltage (log*I*–*V*) characteristics of the Au/Orcein/*p*-Si/Al structure.

good rectifying characteristic. The rectification ratio is about 2×10^3 at ±0.8 V and it shows a good saturated reverse bias current. The values of the n and Φ_b obtained from I–V characteristics using Eqs. (3) and (4) are 2.48 and 0.70 eV, respectively. The value of the ideality factor is greater than unity. The high values in the ideality factor are caused possibly by various effects such as inhomogeneities of Orcein film thickness, interface states, series resistance and non-uniformity distribution of the interfacial charges [14]. Namely, the high ideality factor suggests that the transport properties of the device could not be well defined by thermionic emission only. Higher ideality factor could be due to presence of secondary mechanism at the interface. It is expected that the Orcein organic film forms a physical barrier between the metal and p-Si inorganic substrate, preventing the metal from directly contacting the Si surface. This organic layer appears to cause a significant modification of interface states even though the organic–inorganic interface becomes abrupt and unreactive Thus, the change in barrier height can qualitatively be explained by an interface dipole induced by the organic layer passivation [15,16]. Kampen et al. [17] have observed by photoemission spectroscopy investigations that the S passivation reduces the surface band bending on n-type doped GaAs, and on the other hand, the band bending on the surfaces of p-type doped GaAs increases. Similarly, Zahn et al. [15] have indicated that the initial increase or decrease in effective barrier height for the organic interlayer is correlated with the energy level alignment of the lowest unoccupied molecular orbital (LUMO) with respect to the conduction band minimum of the inorganic semiconductor at the organic–inorganic semiconductor interface.

Furthermore, to understand which mechanisms can control the diode behavior the I–V characteristic of the Au/Orcein/p-Si/Al contact is presented in log–log scale in Fig. 3. In Fig. 3, the forward bias log$I$–log$V$ curve is characterized by two distinct linear regions. At high voltage the current–voltage characteristics of the device are influenced by the transport properties of the organic materials [18,19]. This suggests that the conduction processes occurring in the Orcein film of the Au/Orcein/p-Si/Al contact would be a possible alternative candidate in determining the forward current at the intermediate and high bias voltage [20]. As can be also seen from the double logarithmic forward bias I–V plot in Fig. 3, the injected charge carriers can be proceed through the junction from the moderately doped p-Si into the Orcein material with much lower concentration. At lower voltages, curve is a straight line and agrees with the Ohm's law plot (an Ohmic conduction is evident with a logarithmic slope of ≈1). At very low voltage the injected effective carrier density may be lower than the background thermal carrier density and the current is then ohmic. The ohmic behavior of the I–V characteristics at low voltages is due to existing background doping or thermally generated carriers. In the II region, I–V plots are controlled by the trap-filled case, following the dependence on V. Thus, the transport through the organic Orcein film is governed by the trapped-charge-limited current (TCLC) in the band gap of the Orcein layer. That is, the space charge limited current (SCLC) conduction should become important when the density of injected freecharge carriers is much larger than the thermal-generated free-charge-carrier density. The current density in the first region obeys $J = \frac{9}{8}\varepsilon\mu\theta\frac{V^2}{d^2}$ equation for semiconductors where μ and ε are mobility of the free carrier in organic layer and permittivity of the organic layer, respectively, and θ is trapping parameter. In the second region the current density obeys $J = q\mu N_v\left(\frac{\varepsilon\varepsilon_0}{qN_t}\right)^m\frac{V^{m+1}}{d^{2m+1}}$ equation. Where N_t is the total concentration of traps in the band gap of the organic layer [20,21].

The diffusion potential value of 0.42 V for the device was obtained from the double linear forward bias I–V plot in Fig. 4. This value is in close agreement with the value 0.41 V from the experiment reverse bias C^{-2}–V plot in Fig. 9. The diffusion potential at zero bias which is determined from an extrapolation of the linear C^{-2}–V plot to the V-axis.

For junction devices, the series resistance is an important parameter, affecting the electrical characteristics of Schottky diodes. The Schottky diode parameters such as the barrier height,

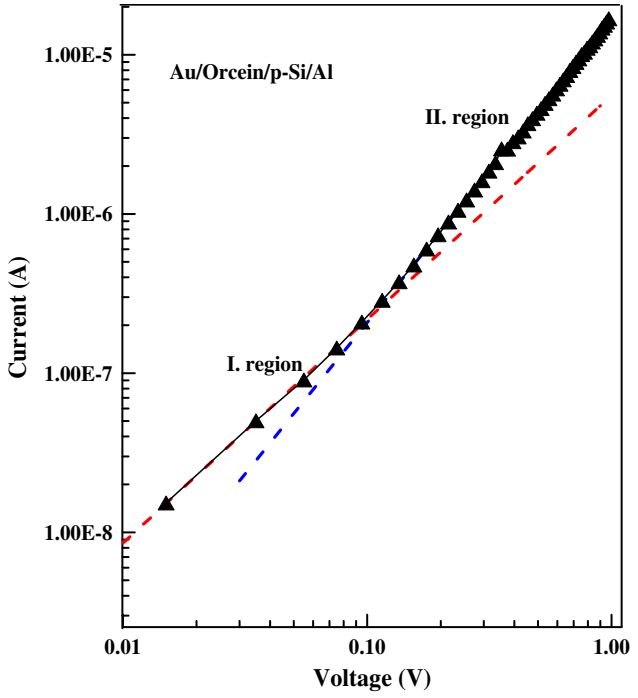

Fig. 3. The forward bias log(I) vs. log(V) plot of the Au/Orcein/p-Si/Al contact from the data in Fig. 2.

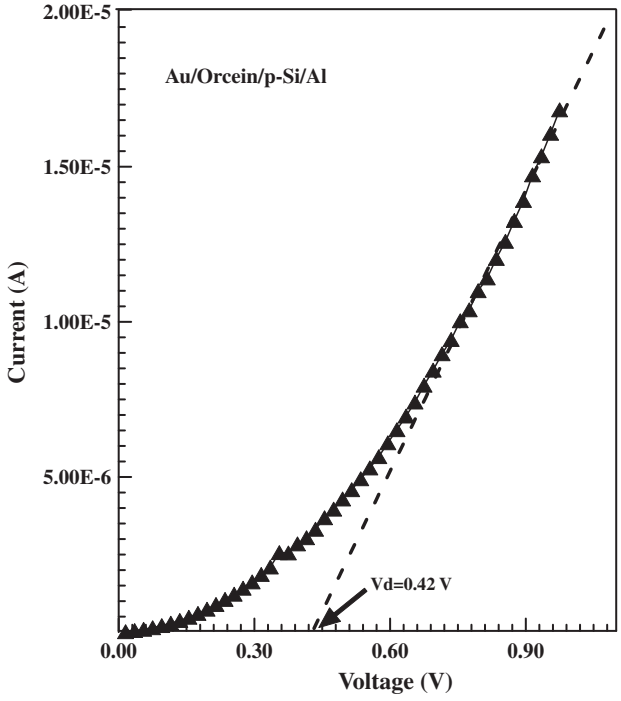

Fig. 4. The forward bias and reverse double linear I–V plot of the Au/Orcein/p-Si/Al device from the data in Fig. 2.

the ideality factor and the series resistance can also be obtained using a method developed by Cheung and Cheung [22]. According to [22], the forward bias I–V characteristics due to the TE of a Schottky diode with the series resistance can be expressed as:

$$I = I_0 \exp\left[\frac{q(V - IR_s)}{nkT}\right], \tag{5}$$

where the IR_s term is the voltage drop across series resistance of device. The values of the series resistance can be determined from the following functions using Eq. (5):

$$\frac{dV}{d(\ln I)} = \frac{nkT}{q} + IR_s, \tag{6}$$

$$H(I) = V - \left(\frac{nkT}{q}\right)\ln\left(\frac{I}{AA^*T^2}\right), \tag{7}$$

and $H(I)$ is given as follows:

$$H(I) = n\Phi_b + IR_s, \tag{8}$$

A plot of $\frac{dV}{d(\ln I)}$ vs. I will be linear and gives R_s as the slope and $\frac{nkT}{q}$ as the y-axis intercept from Eq. (6). Fig. 5 shows the plots of $\frac{dV}{d(\ln I)}$ and $H(I)$ vs. I for Au/Orcein/p-Si/Al structure. From Eq. (6) the values of n and R_s have been calculated as $n = 4.13$, $R_s = 23\ \text{k}\Omega$. Using the value of the n obtained from Eq. (5), the value of Φ_b is obtained from plot of a function $H(I)$ given by Eq. (8). From $H(I)$ vs. I plots, the values of the Φ_b and R_s have been calculated as $\Phi_b = 0.66$ eV, $R_s = 24\ \text{k}\Omega$, respectively. It can be obviously seen that the values of R_s obtained from $H(I)$–I curve are close to the values obtained from the $dV/\text{d}(\ln I)$–I plot.

In the determination the value of the series resistance an alternative method was proposed by Norde [23] as follows:

$$F(V) = \frac{V}{\gamma} - \frac{kT}{q}\ln\left(\frac{I(V)}{AA^*T^2}\right) \tag{9}$$

where γ is an integer (dimensionless) greater than ideality factor. $I(V)$ is current obtained from the I–V curve. Once the minimum of the F vs. V plot is determined, the value of barrier height can be obtained from Eq. (10), where $F(V)$ is the minimum point of $F(V)$ and V_0 is the corresponding voltage

$$\Phi_b = F(V) + \frac{V_0}{\gamma} - \frac{kT}{q} \tag{10}$$

Fig. 6 depicts the $F(V)$–V plot of the structure. From Norde's functions, R_s value can be determined from Eq. (11)

$$R_s = \frac{kT(\gamma - n)}{qI} \tag{11}$$

From the F–V plots the values of Φ_b and R_s of the structure have been calculated as 0.69 eV and 26 kΩ, respectively. It has been seen that the values of the series resistance and barrier height obtained from both Cheung and Norde methods are in agreement with each other. The high value series resistance indicates that the product of the mobility and the free carrier concentration has reduced due to the organic layer and oxide layer at the interface.

For the interface states in equilibrium with the semiconductor, the ideality factor n is given by [24]:

$$n(V) = 1 + \frac{\delta}{\varepsilon_i}\left(\frac{\varepsilon_s}{w} + qN_{ss}(N)\right) \tag{12}$$

where ε_i and ε_s are the permittivities of interfacial layer and the semiconductor, w is the width of the space charge region and N_{ss} is the density of the interface states in equilibrium with the semiconductor. Furthermore, in p-type semiconductors, the energy of the interface states E_{ss} with respect to the top of the valance band at the surface of the semiconductor is given by [25]:

$$E_{ss} - E_v = q\Phi_e - qV \tag{13}$$

The energy distribution or density distribution curves of the interface states can be determined from the experimental data of the forward bias the I–V characteristics. N_{ss} vs. E_{ss}–E_v plots of the Au/Orcein/p-Si/Al Schottky diode are shown in Fig. 7. As can be seen in the figure, exponential growth of the interface state density towards the top of the conduction band is very apparent. It has been seen that the interface state densities have exponential rise with bias towards the top of the valence band. The interface state density N_{ss} obtained from the forward bias I–V ranges from 1.23–$3.44 \times 10^{15}\ \text{cm}^{-2}\ \text{eV}^{-1}$. These changes have been attributed to the decrease in recombination centre and the existence of an interfacial layer between Orcein layer and p-Si semiconductor.

Figs. 8 and 9 show the forward C–V and the reverse bias $1/C^2$–V plots of the contact measured at various frequencies. It can be seen that in reverse bias the value of the capacitance is almost constant

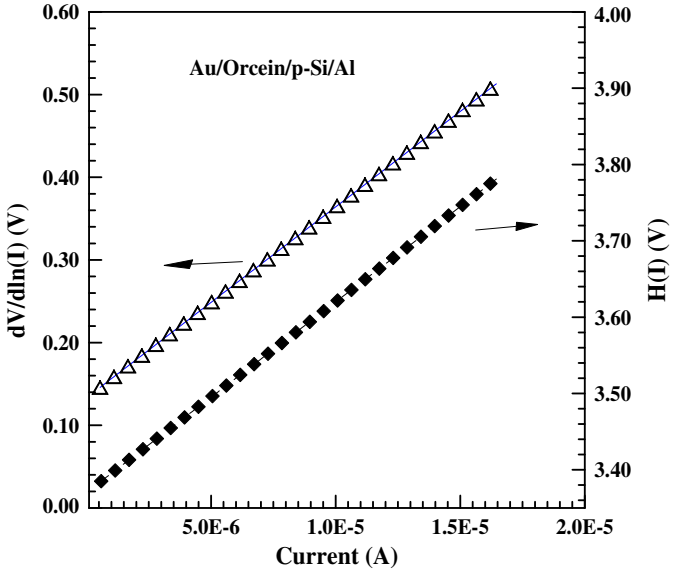

Fig. 5. A plot of $\frac{dV}{d(\ln I)}$ vs. I and $H(I)$ vs. I obtained from forward bias current–voltage characteristics of the Au/Orcein/p-Si/Al structure.

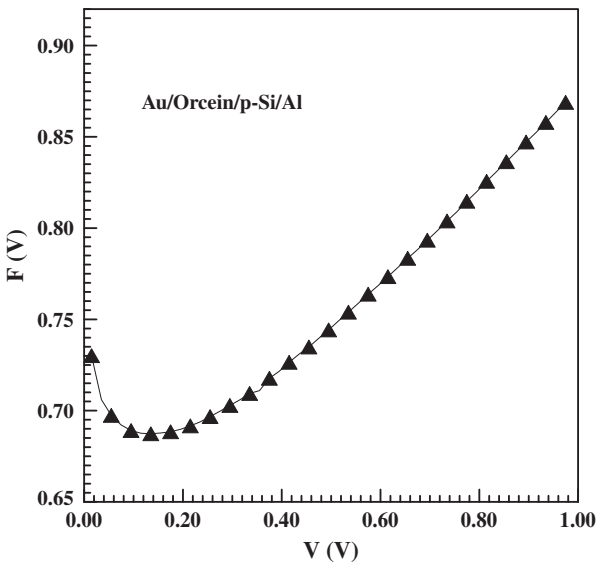

Fig. 6. $F(V)$ vs. V plot of the Au/Orcein/p-Si/Al structure.

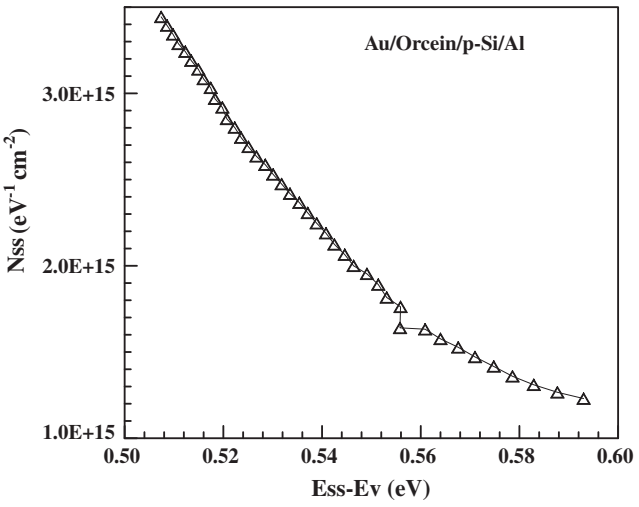

Fig. 7. *Nss* vs. E_{ss}–E_v plots of the Au/Orcein/*p*-Si/Al Schottky diode.

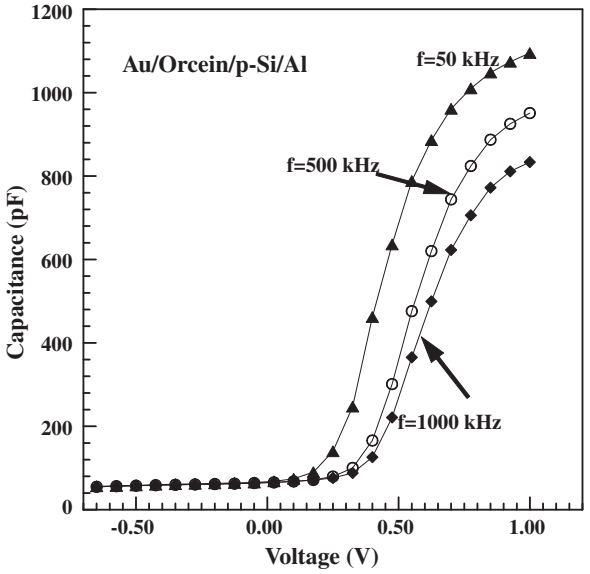

Fig. 8. The forward bias *C*–*V* characteristics of the Au/Orcein/*p*-Si/Al device at various frequencies.

and it is sharply increasing in forward bias towards high voltages. The higher values of capacitance at low frequency are due to the excess capacitance resulting from the interface states in equilibrium with the *p*-Si that can follow the alternating current (a.c) signal. Namely, the interface states at lower frequencies follow the a.c signal, whereas at higher frequencies they cannot follow the alternating current signal. The diffusion potential at zero bias which is determined from an extrapolation of the linear C^{-2}–*V* plot to the *V*-axis as 0.41 V. In metal/semiconductor contacts the depletion layer capacitance is given as follows [2],

$$C^{-2} = \frac{2(V_d + V)}{\varepsilon_s \varepsilon_0 q A^2 N_A} \tag{14}$$

where V_d is the diffusion potential at zero bias which is determined from the extrapolation of the linear $1/C^2$–*V* plot to the *V*-axis, *A* is the effective area of the diode and ε_s is the dielectric constant of the semiconductor (=11.7 for Si) [2], ε_0 is the dielectric constant of vacuum (=8.85 × 10^{-14} F/m) and N_A is the concentration of ionized acceptors and it is written as:

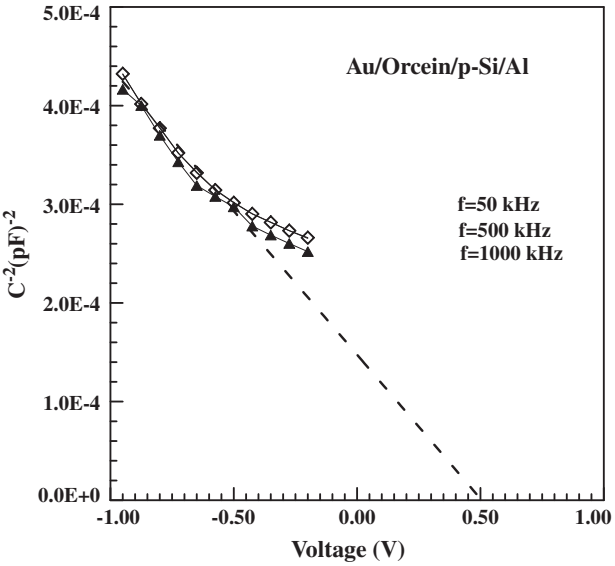

Fig. 9. The reverse bias C^{-2}–*V* characteristics of the Au/Orcein/*p*-Si/Al structure at various frequencies.

$$N_A = N_V \exp(V_p/kT) \tag{15}$$

The acceptor concentration has been found as 6.65 × 10^{14} cm^{-3} by using $1/C^2$–*V* plot at *f* = 500 kHz. At the high frequencies, the values of the capacitance are only space charge capacitance. From the capacitance–voltage measurements the values of the barrier heights were calculated as 0.81 at *f* = 500 kHz. The *C*–*V* curves gave a Schottky barrier height (BH) value higher than those derived from the *I*–*V* measurements. This discrepancy can be explained by the different nature of the *C*–*V* and *I*–*V* measurement techniques. Barrier heights deduced from two methods are not always the same. If the barriers are uniform and ideal, the two measurements yield the same value; otherwise, they will yield different values. The different behavior of BHs obtained from the two techniques can be explained by a distribution of BHs due to the inhomogeneties (as a combination of the interfacial oxide layer composition, non-uniformity of the interfacial Orcein layer thickness, and distribution of interfacial charges) that occur at metal/semiconductor interface [26].

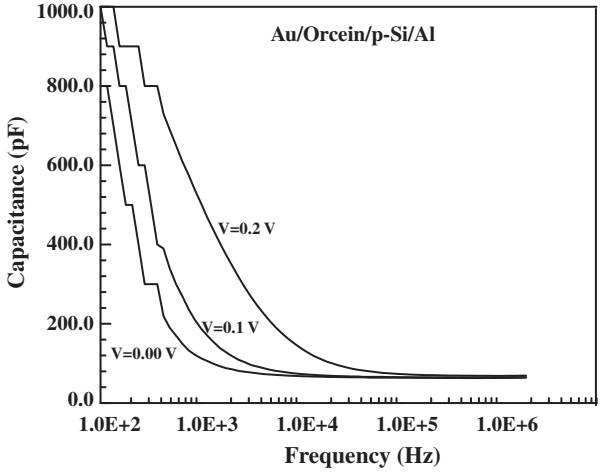

Fig. 10. The forward bias *C*–*f* characteristics of the Au/Orcein/*p*-Si/Al structure at various voltages.

Fig. 10 shows the capacitance–frequency (C–f) characteristics of the Au/Orcein/p-Si/Al device at various voltages. According to the Fig. 9, when the frequency is increased, the capacitance shows strong frequency dependence and tends to decrease rapidly. The values of the capacitance at the high frequency region originate from only space charge capacitance at higher frequencies since they cannot follow the alternating current signal. Generally, the capacitance measured for a Schottky diode is dependent on the reverse bias voltage and frequency. The voltage and frequency dependence is due to the particular features of a Schottky barrier, impurity level, high series resistance, etc. As the frequency is increased, the total diode capacitance is affected not only by the depletion capacitance, but also by the bulk resistance and associated with hole or electron emission from slowly responding deep impurity levels [2,27].

4. Conclusions

The experimental I–V, C–V, and C–f characteristics of the Au/Orcein/p-Si/Al contact have been studied. Various junction parameters e.g. ideality factor, barrier height, and series resistance has been calculated. Under forward bias conditions, ohmic and TCLC conductions have been identified at low and higher voltages, respectively. The interface state density of the Au/Orcein/p-Si/Al contact has been also calculated and these values have ranged from $1.23–3.44 \times 10^{15}\ \mathrm{cm^{-2}\ eV^{-1}}$. The experimental values of the capacitance have modified with bias and frequency.

References

[1] T. Maeda, S. Takagi, T. Ohnishi, M. Lippmaa, Mater. Sci. Semicond. Process. 9 (2006) 706–710.
[2] E.H. Rhoderick, R.H. Williams, Metal-Semiconductor Contacts, second ed., Clarendon Oxford, 1988.
[3] R.K. Gupta, K. Ghosh, P.K. Kahol, Physica E 41 (2009) 876.
[4] R.K. Gupta, K. Ghosh, P.K. Kahol, Curr. Appl Phys. 9 (2009) 933.
[5] R.K. Gupta, K. Ghosh, P.K. Kahol, Physica E 41 (2009) 1201.
[6] S. Aydogan, M. Saglam, A. Turut, Vacuum 77 (2005) 269.
[7] S. Aydogan, M. Saglam, A. Turut, Polymer 46 (2005) 563.
[8] M. Cakar, N. Yildirim, S. Karatas, C. Temirci, A. Turut, J. Appl. Phys. 100 (2006) 074505.
[9] A.R.V. Roberts, D.A. Evans, Appl. Phys. Lett. 86 (2005) 072105.
[10] S. Karatas, A. Turut, Vacuum 74 (1) (2004) 45.
[11] J.C. Scott, J. Vac. Sci. Technol., A 21 (2003) 521.
[12] I. Kymissis, C.D. Dimitrakopoulos, S. Purushothaman, IEEE Trans. Electr. Devices 48 (2001) 1060.
[13] W. Brütting, Physics of Organic Semiconductors, WILEY-VCH Verlag GmbH and Co. KGaA, Weinheim, 2005.
[14] O. Güllü, S. Aydoğan, A. Türüt, Microelectron. Eng. 85 (2008) 1647–1651.
[15] D.R.T. Zahn, T.U. Kampen, H. Mendez, Appl. Surf. Sci. 212–213 (2003) 423.
[16] A. Bolognesi, A. Di Carlo, P. Lugli, T. Kampen, D.R.T. Zahn, J. Phys.: Condens. Matter 15 (2003) S2719.
[17] T.U. Kampen, A. Schuller, D.R.T. Zahn, B. Biel, J. Ortega, R. Perez, F. Flores, Appl. Surf. Sci. 234 (1–4) (2004) 341.
[18] S.R. Forrest, P.H. Schmidt, J. Appl. Phys. 59 (1986) 513.
[19] R.K. Gupta, K. Ghosh, P.K. Kahol, Physica E 42 (2010) 1509.
[20] M.E. Aydin, A. Türüt, Microelectron. Eng. 84 (2007) 2875.
[21] S.R. Forrest, Chem. Rev. 97 (1997) 1793.
[22] S.K. Cheung, N.W. Cheung, Appl. Phys. Lett. 49 (1986) 85.
[23] H. Norde, J. Appl. Phys. 50 (1979) 5052.
[24] J.C. Card, E.H. Rhoderick, J. Phys. D 4 (1971) 1589.
[25] A. Singh, Solid-State Electron. 28 (1985) 233.
[26] C. Coskun, S. Aydogan, H. Efeoglu, Semicond. Sci. Technol. 19 (2) (2004) 242.
[27] Suresh C. Jain, M. Willander, Vikram Kumar, Conducting Organic Materials and Devices, Elsevier Academic Press, The Netherlands, 2007.